Tunneling properties of $Al_xGa_{1-x}As$ and AlAs barriers studied by ballistic electron luminescence spectroscopy

M. V. Petrov, S. R. Parihar,* and S. A. Lyon
Department of Electrical Engineering, Princeton University, Princeton, New Jersey 08544
(Received 12 March 1996)

Tunneling through barriers of $Al_xGa_{1-x}As$ and AlAs was studied using ballistic electron luminescence spectroscopy. The luminescence provides information on the energy distribution of the carriers after they have exited the barrier and are injected into GaAs. For electron tunneling through $Al_xGa_{1-x}As$ ($x \leq 0.3$) barriers good agreement with a simple theory is obtained. The behavior of AlAs barriers is more complicated and can be explained only by assuming incoherent tunneling of electrons when their energy is above the X-point conduction band of the AlAs barrier. Hole tunneling is also observed, and the hole tunneling current is comparable to the electron current under appropriate conditions. [S0163-1829(96)01843-7]

I. BALLISTIC ELECTRON LUMINESCENCE SPECTROSCOPY

Experimental measurement of the energy distribution of nonequilibrium electrons is a direct way for understanding the nature of tunneling through complex semiconductor barriers. Progress has been made recently in designing hot-electron transistors and other electrical devices[1,2] where electrons are injected ballistically by using heterojunctions. On the other hand, optical experiments have been proven to be useful for measuring nonequilibrium energy distributions and their evolution in time.[3] While electrical transport experiments are precise for measuring integrated characteristics of a device, determining the energy distribution of injected electrons is usually not a straightforward problem. Among the intriguing observations is, for example, negative differential resistivity of a single AlAs barrier.[4] Ballistic electron luminescence spectroscopy (BELS) Ref. 5 is a useful tool for investigating the problem and combining the practicality of electrical measurements with the precision of measuring carrier distributions inherent in optical experiments.

Ballistic electron luminescence spectroscopy is an optical technique for studying highly nonequilibrium transport. The basic idea of BELS is illustrated in Fig. 1. Electrons are injected into p-doped GaAs and allowed to recombine with holes at neutral acceptors, producing light at wavelengths corresponding to the electron energies. Ballistic electron recombination with thermalized holes in the **p** layer is forbidden by momentum conservation. When the experiments are done at temperatures below about 40 K, the Be acceptors (29 meV deep[6]) are frozen out (neutral) and radiative recombination of a large momentum electron and the localized hole becomes possible. The beam of ballistic electrons can be created by a potential energy profile discontinuity in the conduction band of an $Al_xGa_{1-x}As$/GaAs heterodiode, as shown in Fig. 1. Under forward bias electrons are injected into the lightly doped **p**-type region. The recombination probability of a ballistic electron with neutral acceptors is very low,[7] so that only a negligible (about 10^{-6}) fraction of the electrons is lost. Thus the radiative process does not change the dynamics of hot carriers and can be used to measure the hot electron energy distribution. The radiative recombination rate is a smooth function of electron energy, so that peaks in the luminescence spectrum represent peaks in the electron energy distribution averaged over sample thickness.

As shown in Fig. 2, a BELS spectrum exhibits a sequence of peaks separated by the LO phonon energy, about 37 meV. The highest energy peak is ascribed to ballistic electron recombination with neutral acceptors. The second highest energy peak is due to electrons which have emitted one LO phonon and then recombined. Up to eight phonon repetitions of the main ballistic peak have been observed. The low energy lines in this series are obscured by the GaAs band-edge luminescence. As noted earlier, very few electrons recombine while they are hot. Nearly all thermalize to the conduction-band edge, where they recombine with free and bound holes. The spectrum rises approximately exponentially as the band gap (about 1.52 eV) is approached from above. The rising tail of the band-edge luminescence usually

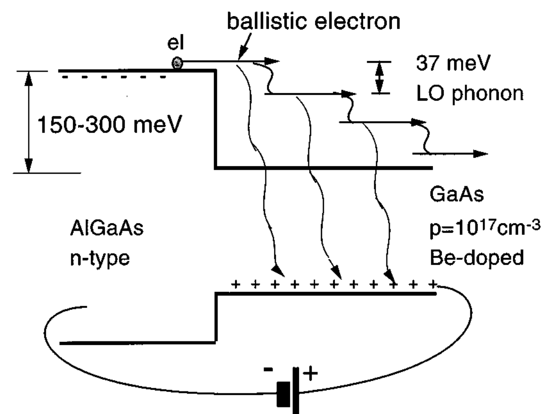

FIG. 1. Schematic of a BELS experiment with heterojunction as an injector of ballistic electrons. The **p** layer is moderately doped (10^{17} cm^{-3}) so that the acceptors are frozen out at low temperatures. The applied voltage flattens the bands and injects electrons from $Al_xGa_{1-x}As$ into GaAs, where they can radiatively recombine with neutral acceptors. The electron energy is determined by the conduction-band offset of the heterojunction.

 © 1996 The American Physical Society

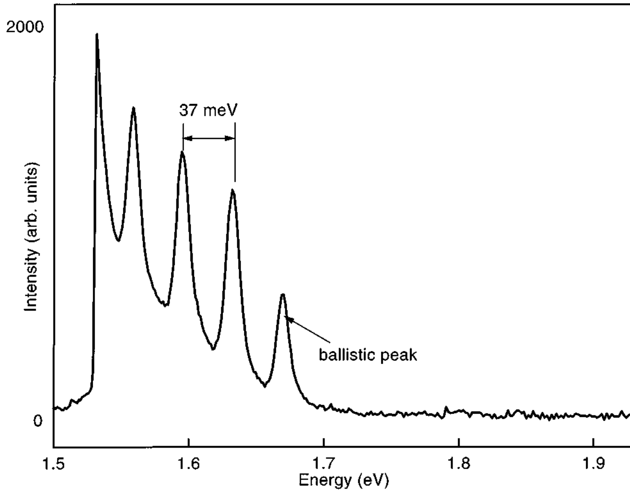

FIG. 2. A BELS spectrum obtained on a sample with a $Al_xGa_{1-x}As/GaAs$ heterojunction as an injector of ballistic electrons. The highest energy peak is due to ballistic electron recombination with neutral acceptors. The lower energy peaks are phonon repetitions of the ballistic electron peak. These peaks are due to recombination of electrons which have emitted one or more optical phonons.

makes it impossible to reliably measure ballistic peaks with energy less than about 50 meV.

In comparison with simple heterojunctions, tunnel injectors offer the advantage of tuning the electron energy by changing applied voltage. The electrons are injected through a tunnel barrier into a lightly **p**-doped GaAs layer, where they can recombine, emitting photons with the energy determined by the electron kinetic energy. Thus, the information on the electron energy and distribution is obtained for different voltages across the barrier.

Recently BELS was implemented for studies of double-barrier resonant tunneling structures[8] and single-barrier $Al_xGa_{1-x}As$ heterostructures.[9,10] For the double-barrier structure the ballistic currents from two confined electron states were quantitatively determined. In the studies of single-barrier structures in a magnetic field the splitting of the electron and hole accumulation regions into well defined confined states was seen.

This paper is organized as follows. In Sec. II we will give a brief overview of calculations of tunneling current through $Al_xGa_{1-x}As$ and AlAs barriers. In Sec. III the details of the experiments will be described. Following it, Sec. IV presents the BELS spectra for $Al_xGa_{1-x}As$, AlAs, and composite barrier samples. A discussion and interpretation of the spectral data will be given in Sec. V. Finally, in Sec. VI we demonstrate that the hole tunneling can also be important and determine what fraction of the total current is due to electrons, and what fraction is holes. A four-terminal device was used in these experiments.

II. THEORETICAL BACKGROUND

We have performed calculations of the current versus voltage (I-V curves) for the different samples used in the experiment. The calculations were based on the parameters in Table I. Illustrated in Fig. 3 is a schematic of the band

TABLE I. Heterojunction parameters.

	GaAs	AlAs
E_X^0 (eV)	0.480[a]	0.170[b]
E_Γ^0 (eV)	0.0	1.11[b]
E_L^0 (eV)	0.32[c]	0.33[c]
Δ (eV)	0.35[d]	
$m_\Gamma(m_0)$	0.067[a]	0.15[a]
$m_X(m_0)$	1.9[a]	1.32[a]
$m_{\mathrm{lh}}(m_0)$	0.08[a]	0.16[a]
$m_{\mathrm{hh}}(m_0)$	0.55[a]	0.81[a]

[a]Reference 6.
[b]Reference 12.
[c]Reference 11.
[d]Reference 3.

bending when voltage is applied to a tunnel barrier structure. While the bias flattens the lightly doped n and p layers, the applied voltage causes accumulation layer formation and the barrier to tilt. In the effective mass approximation the tunneling probability for a triangular barrier is given directly by a single formula.[13] Although appropriate for rough estimates, the WKB method gives up to a factor of 2 error in finding the tunneling coefficient, and it has not been used. The accumulation regions are treated with a classical Poisson equation, assuming that the subband structure in the accumulation layers should not dramatically affect the tunneling current. Under typical experimental conditions, an accumulation region can contain up to about 10^{12} cm^{-2} carriers. Depending on the background doping, the subbands of that 2D electron layer could be well separated and distinct for experiments done at 5–10 K. Thus a more elaborate theory of tunneling would involve a simultaneous solution of the Poisson and Schrödinger equations to find the tunneling current from all subbands. At the same time, our estimates show that our errors in current calculations due to the use of a classical

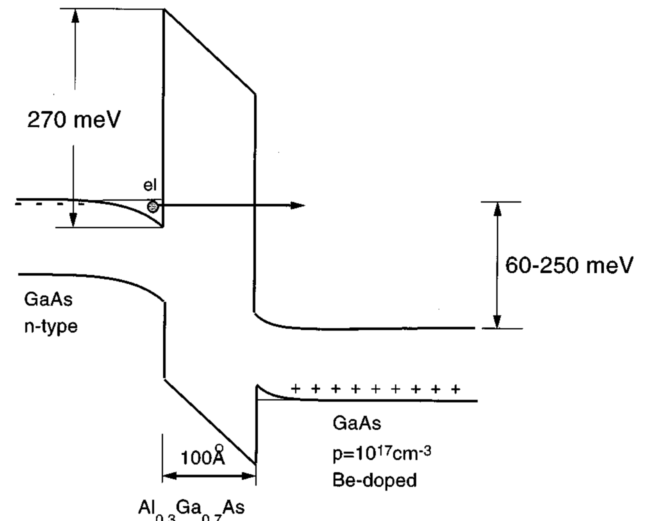

FIG. 3. Schematic band diagram of an $Al_xGa_{1-x}As$ tunnel barrier BELS device. When the diode is forward biased at low temperature, electrons are tunnel-injected into the **p**-GaAs. The kinetic energy of these electrons can be tuned with the applied voltage.

model are comparable with other errors due to uncertainties in material parameters. Taking into account that, as in any tunneling process, the calculated rates depend exponentially on the assumed thickness of the barrier and material parameters, the use of a quantum theory of accumulation regions in our case would exceed the precision with which the system parameters are known.

In $Al_xGa_{1-x}As$ ($x \leqslant 0.3$) the conduction-band minimum belongs to the Γ valley, so that a tunneling electron goes from the Γ valley in GaAs through the Γ valley of $Al_xGa_{1-x}As$, and back to the Γ valley in GaAs. Because no intervalley mixing is involved, the tunneling probability is not reduced compared with a simple quantum-mechanical probability of tunneling through a potential barrier. This case is well understood theoretically and experimentally (for example, see Ref. 14) and serves as a good test of our technique.

The tunneling through AlAs barriers is qualitatively different from the tunneling in $Al_xGa_{1-x}As$ ($x \leqslant 0.3$). The main difference is that AlAs is an indirect material with its conduction-band minimum lying towards the X point, while GaAs is a direct material with a Γ minimum of the conduction band. For a single AlAs barrier we have performed calculations following the method cited in Ref. 15. We assumed a 170 meV band offset for the X valley in AlAs to the GaAs conduction-band edge and the electron mass of $1.32m_0$ in AlAs. The band offset for the Γ valley was taken as 1.1 eV with an electron mass of $0.15m_0$, as shown in Table I. While the applied voltage is less than X valley energy in GaAs, the tunneling should bring a Γ electron from the GaAs injector side to a Γ state in the GaAs collector. An electron can tunnel through two channels in the AlAs: $\Gamma \rightarrow X \rightarrow \Gamma$ and $\Gamma \rightarrow \Gamma \rightarrow \Gamma$. higher The $\Gamma \rightarrow X \rightarrow \Gamma$ channel is energetically preferable. However, that channel requires wave-function conversion between X and Γ Bloch states. Tunneling through this channel is suppressed by the weak coupling between the X and Γ states.[15,16] So the question arises which channel the electron tunnels through, whether it is $\Gamma \rightarrow X \rightarrow \Gamma$, $\Gamma \rightarrow \Gamma \rightarrow \Gamma$, or a superposition of the two. In general, $\Gamma \rightarrow \Gamma \rightarrow \Gamma$ channel goes through a continuum of states because the electron energy never exceeds 1.11 eV Γ offset energy in AlAs, while $\Gamma \rightarrow X \rightarrow \Gamma$ channel, when the electron energy gets higher than 190 meV, proceeds through a set of discrete states. If intensities of the two channels are comparable, then Fano-type resonances are predicted[17] for the tunneling probability function.

III. EXPERIMENTAL METHOD

The samples were grown on [001] GaAs substrates by molecular beam epitaxy and processed using standard wet etching techniques. In the design of a BELS device the thickness of the **p**-layer is usually made commensurate with the scattering lengths of the electrons in order to maximize the optical signal of ballistic electrons and minimize the background. This sets the typical thickness of a sample to a few thousand angstroms. All active layers were contacted individually. We used 100–200 μm mesas. The wet etching was done with a nonselective H_3PO_4 etch. For n-type contacts we used a AuGe (90:10) alloy deposited on a 50 Å Ti film; p-type contacts were made of 50 Å layer of Ti, 100 Å Zn, and capped with gold. Later the contacts were alloyed at 400 °C for 20 sec, and gold leads were attached using a wire bonder. The samples were mounted in a liquid He optical dewar. Luminescence spectra were taken with a Spex Triplemate spectrometer equipped with a liquid nitrogen cooled CCD system. The weakest signals required integration times of up to a few hours for a single spectrum.

Particular attention was given to the crystal growth, because our devices had a relatively large area and because vertical transport devices are generally very sensitive to structural defects. The requirements to obtain good optical and electrical quality in thick $Al_xGa_{1-x}As$ layers has led us to employ high (to 700 °C) substrate temperature and reduced As:Ga flux ratio. For the tunnel barrier structures (with only thin $Al_xGa_{1-x}As$ layers) regular GaAs growth conditions (T_{sub} typically 600 °C) were used. Especially damaging to the performance of a device were oval defects.[20] Usually devices containing even a single oval defect drove a good fraction of the total current through the defect, as could be observed by looking at the band-edge electroluminescence of the sample. The defect appeared as a bright spot on a darker background. Spectra of oval defects usually do not reveal any hot carrier structure. To reduce the possibility of band bending due to dopant diffusion, all the structures reported here were grown with a Be-doped region on top of Si-doped layers. Also, 100 Å spacers on both the **p** and **n** sides of the tunnel barrier were inserted.

Typical current densities in these experiments were relatively low. The maximum current density did not exceed

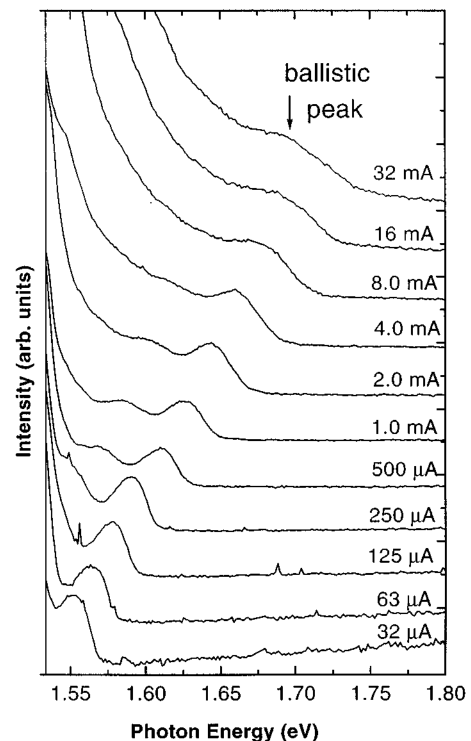

FIG. 4. BELS spectra of an $x=0.3$ 100 Å tunnel barrier sample obtained at different currents through the sample. On the spectra a ballistic peak and one or two of its phonon repetitions are observed. The broadening seen at high currents is a result of the increasing depth of the electron accumulation layer in the injector.

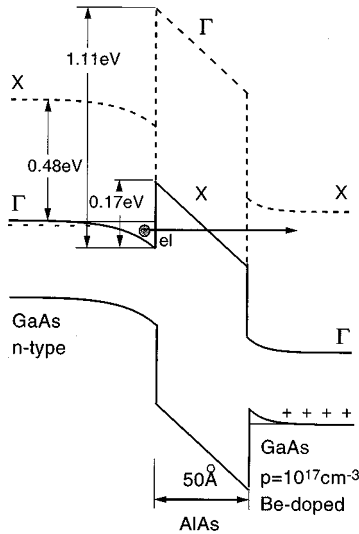

FIG. 5. Schematic band diagram of the AlAs tunnel barrier sample. The AlAs is indirect, with its conduction-band minimum near the X point. The bulk AlAs X point lies below the GaAs X point, leading to quasibound states in the AlAs. With sufficient applied voltage, the tunneling electron's energy can lie above the conduction-band minimum in the AlAs, as shown.

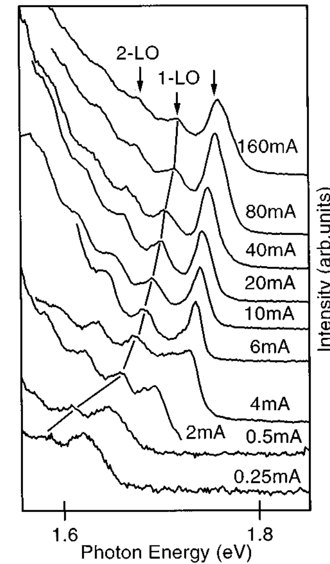

FIG. 6. BELS spectra of AlAs barrier sample. Note that the highest energy peak changes its structure at about the 2 mA current level. It becomes sharper, while its separation from the phonon series grows from about 37 meV to 45 meV.

6×10^2 A/cm^2. The escape time of an electron from the GaAs/AlAs/GaAs X-valley quantum well is thought to be about 1 psec,[21] so that the carrier density inside the barrier does not exceed 4×10^9 electrons/cm^2. Even in this worst case the electron density is still considerably lower than the electron concentration in the accumulation region (up to about 2×10^{12} electrons/cm^2, as follows from a solution of the Poisson equation for a typical bias across the barrier). This estimate shows that electron accumulation inside the barrier can be neglected for calculating total band bending.

IV. EXPERIMENTAL DATA

A. Tunneling through $Al_xGa_{1-x}As$

We have studied the tunneling through simple $Al_xGa_{1-x}As$ barriers with a variety of barrier parameters. The bands for an $x=0.3$, 100 Å barrier sample are shown schematically in Fig. 3. The voltage is applied between the top and the bottom layers. The electrons are injected from the $n=10^{17}$ cm^{-3} Si-doped emitter into the $p=1.5\times10^{17}$ cm^{-3} Be doped region, where they can radiatively recombine with neutral acceptors. Electroluminescence spectra of this sample at a variety of currents are shown in Fig. 4. The spectra exhibit one or more peaks separated by about 37 meV, the LO phonon energy. Such a series of peaks separated by the LO phonon energy is indicative of energetic electrons being injected into and then relaxing in the GaAs. The highest energy peak corresponds to recombination of ballistic electrons and the energy with which the electrons have been injected is given directly by the photon energy. As the current (applied voltage) increases, the peaks shift towards higher energy. The ballistic peak also broadens considerably at high currents as the depth of the electron accumulation layer in the emitter grows. In this sample the injection energy can be tuned from 70 meV up to about 250 meV.

B. AlAs barrier tunneling

The simplest of our AlAs-containing structures was a single pure AlAs barrier. The thickness of 50 Å was found to give a reasonable tuning range of the electron energy in the BELS experiments. The band diagram is sketched in Fig. 5. Of particular importance, as will be discussed in detail below, is the fact that AlAs is indirect with its conduction band edge at the X point. Similar to the $Al_xGa_{1-x}As$ samples described above, the 50 Å barrier AlAs sample contained an **n**-doped ($n=2\times10^{17}$ cm^{-3}) injector region, undoped barrier, and a **p**-doped ($p=1\times10^{17}$ cm^{-3}) collector. The BELS spectra for the AlAs barrier are shown in Fig. 6. At low currents (below about 2 mA) the spectra look similar to the earlier ones for the simple $Al_xGa_{1-x}As$ barriers—a series of peaks separated by the LO phonon energy. At about 6 mA, however, the highest energy peak begins to grow and become narrower. This is in contrast to the broadening seen at higher currents in the $Al_xGa_{1-x}As$-barrier structures. This peak is also more than one LO phonon energy above those labeled "1-LO," which correspond to injected electrons which have emitted a single LO phonon. The actual ballistic peak is barely visible as a low-energy shoulder on this sharp line in the 6 mA spectrum.

C. Composite barriers

Another set of samples was studied in order to probe deeper into the tunneling mechanisms in AlAs. We have designed composite barrier structures, a combination of an $Al_xGa_{1-x}As$ and an AlAs barrier. In these structures an electron tunnels through the $Al_xGa_{1-x}As$ barrier before it is injected into AlAs, as shown in Fig. 7. The composite barri-

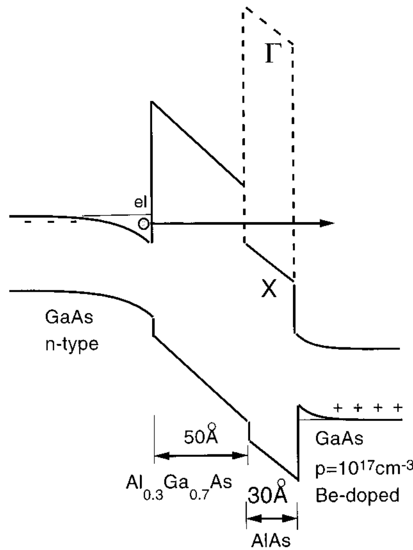

FIG. 7. Schematic band diagram of the composite barrier structure. Electrons tunnel through $x=0.3$ $Al_xGa_{1-x}As$ barrier before entering the AlAs. This allows the injection of an electron with different energies into AlAs.

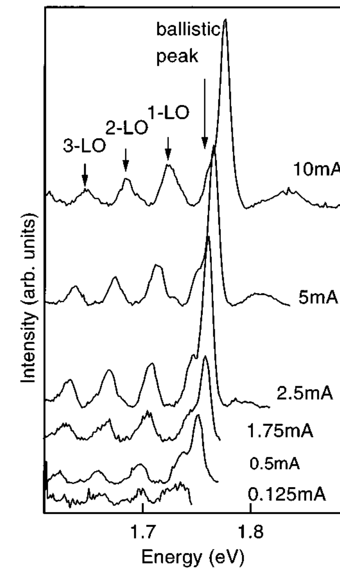

FIG. 8. BELS of the thinner composite barrier sample. In addition to the optical phonon sequence, a sharp peak is seen at an energy exceeding the ballistic peak energy by about 10 meV.

ers allow the tunneling electrons to enter either above or below the X-point minimum of the AlAs, depending upon the sample structure and applied bias. Described here are the data obtained with two composite barrier samples which differ in their $Al_xGa_{1-x}As$ layer thicknesses and composition (a third composite barrier structure, a four-terminal device, will be discussed in Sec. VI). The band digram of the first sample is shown in Fig. 7. Here an electron is forced to tunnel through a 50 Å $Al_{0.3}Ga_{0.7}As$ barrier before its injection into the 30 Å AlAs. The BELS spectra are plotted in Fig. 8. At the lowest current, a ballistic peak and LO phonon series can be seen. However, the higher current spectra are dominated by a sharp line near 1.78 eV, like that seen in Fig. 6 for the simple AlAs barrier. Here the actual ballistic peak can still be seen as a clear low-energy shoulder on the larger peak until the highest currents, and the LO phonon series is very evident. In addition, these spectra show a new line appearing at higher energy than the dominant sharp one, and moving higher with increasing current.

The second composite barrier sample had a 100 Å $Al_{0.3}Ga_{0.7}As$ layer and the same 30 Å AlAs layer. At all currents the injection energy should be higher for this thicker barrier device. Another difference between the two composite barrier samples is in the **p**-layer doping level. The second, thicker sample has a 4000 Å $\mathbf{p}=1\times10^{17}$ cm^{-3} layer, while the thinner one has a higher doping ($\mathbf{p}=2\times10^{17}$ cm^{-3}). The lower doping in the thicker structure should enhance the luminescence of other recombination processes (recombination in the barrier, ballistic hole recombination) relative to the intensity of the ballistic electrons injected into the GaAs and the LO phonon series.

The changes in the structure are evident in the electroluminescence spectra for the thicker composite barrier shown in Fig. 9. Even at the lowest current the spectrum is dominated by the sharp peak near 1.78 eV. A ballistic peak is never evident, even as a shoulder, though the LO phonon series can be clearly seen at higher currents. With the higher injection energies possible in this sample, the broad peak appearing above 1.8 eV in Fig. 8 can now be seen to continue to move up with increasing voltage. However, it splits with one peak remaining nearly constant at about 1.87 eV, and the other reaching about 1.95 eV at our highest current. As discussed in Sec. VI we believe that these high energy peaks arise from hole tunneling and recombination in the n-GaAs.

V. DISCUSSION

A. Tunneling through $Al_xGa_{1-x}As$

The theoretical calculations of tunneling were based on parameters from Table I with the following additional parameters: the conduction-band offset of an $Al_xGa_{1-x}As$/GaAs heterojunction is taken to be $1.453\times0.6x$ (eV) and the electron mass in $Al_xGa_{1-x}As$ is $0.0657+0.0174x+0.145x^2(m_0)$.[6] Given the exponential dependence of tunneling on the barrier thickness, the calculated tunneling probability is very sensitive to the numerical value of the layer thickness. However, the actual MBE-grown 100 Å $Al_xGa_{1-x}As$ layer is uncertain to about 10% in thickness and composition unless special steps are taken. This contributes up to a factor of 3 error in matching experimental and calculated I-V curves. A more useful comparison can be made to the argument of the exponential in the tunneling calculation, which corresponds to the slope of the I-V curve when the current is plotted on a logarithmic scale.

The $x=0.3$ 100 Å barrier sample has tunneling parameters such that a few hundred millivolt voltage drop across the barrier is achieved at a moderate current level, where the optical signal is well detectable but the Joule heating is still negligible. The energy of the ballistic peak measures the true voltage drop across the barrier, allowing us to obtain an ''optical'' I-V curve by plotting current versus ballistic peak energy. The peak energies were taken from the spectra in Fig. 4. This optical I-V curve, along with the calculated I-V

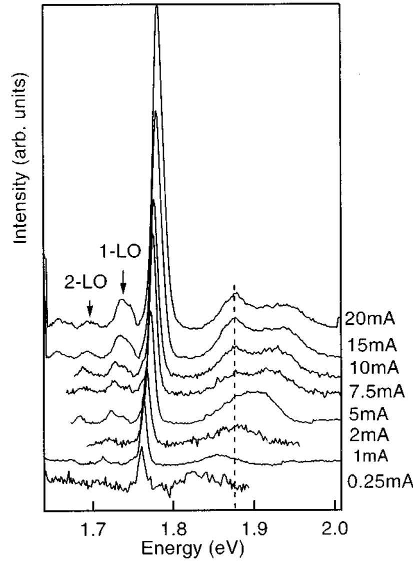

FIG. 9. BELS spectra of the thicker composite barrier sample. The decreased intensity of the phonon sequence, as compared with the sample in Fig. 8, is due to lower acceptor concentration. The higher energy broad peaks do not have any phonon repetition structure.

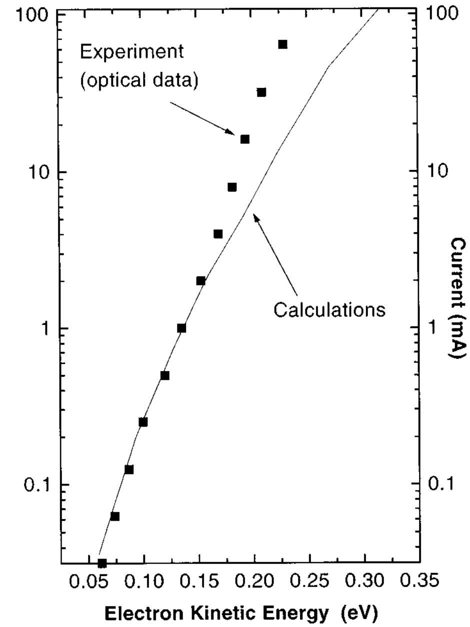

FIG. 10. The optical *I-V* curve of the 100 Å $Al_{0.3}Ga_{0.7}As$ barrier sample. The curve is obtained by plotting the current through the device versus the ballistic peak position measured relative to the cold electron–neutral acceptor luminescence line on the spectra of Fig. 4. The calculated curve is obtained using a simple tunneling theory and parameters as discussed in the text.

curve, is plotted in Fig. 10. The almost perfect match at low currents is fortuitous, given the uncertainty in sample parameters as noted above. However, we typically find less than a factor of 3 discrepancy in the absolute current between measurements and calculations for the simple $Al_xGa_{1-x}As$ barriers. The origin of the discrepancy between the experimental data and the calculations at larger currents is not clear. Joule heating may be involved, because some fraction of the current can be attributed to thermionic injection through the barrier. The peak broadening at high currents agrees well with the assumption that the number of electrons in the accumulation region increases. For example, the ballistic peak width at the 8 mA spectrum is about 30 meV and its energy is about 1.66 eV. This means that the electron kinetic energy, as determined by the total voltage applied to the sample, is about 170 meV. As can be shown by solving the Poisson equation, this voltage corresponds to about 8×10^{11} cm^{-3} carriers in the accumulation layers. Such a carrier density in a 2D electron gas implies about a 30 meV Fermi energy,[22] in agreement with the broadening of the ballistic peak.

B. AlAs barrier tunneling

The spectra of the 50 Å AlAs barrier sample (Fig. 6) show that the ballistic peak tunes to higher energy with increasing current. However, in contrast with the $Al_xGa_{1-x}As$ samples discussed above, the energy tuning rate is faster at low currents, but it becomes much slower at higher currents. Since the ballistic peak is obscured by the sharp 1.78 eV peak at higher currents, we measured the position of the "1-LO" peak and then added the LO phonon energy to obtain the "optical voltage." These data (accumulated from several pieces of the same wafer) are shown in Fig. 11 and clearly demonstrate a kink in the *I-V* curve at approximately 1 mA (current density 4.4 A/cm^2). Under no conditions did the optical voltage go higher than 250 meV above the band gap. This behavior is puzzling as simple theories predict that the ballistic electron energies should continue to increase regardless of whether the electron tunneled through Γ or X states. Although some fluctuations in the transmission function may be expected due to Fano resonances,[17–19] after averaging over the width of our lines, the transmission should increase smoothly, and not change dramatically at a ballistic electron energy of 230 meV.

When the ballistic peak stops increasing in energy, a sharper peak emerges at about 10 meV above the ballistic energy, as noted above. The sharpness of the peak is such that it cannot be explained as coherent electron tunneling from the electron accumulation region, because the accumulation region energy broadening is as large as tens of meV. Also, the peak appears only when the ballistic electron energy exceeds 200 meV. The sharpness of the peak, its energy, and its threshold nature suggest that it originates from electrons in the X-valley quantum well in the AlAs recombining with holes in the adjacent accumulation layer in the GaAs.

We have made several measurements and confirmed this hypothesis. First, we checked whether the peak intensity depends on the **p**-layer thickness by etching part of it away. The intensity of the phonon series dropped, while the intensity of the 1.78 eV peak remained the same. Next, we grew a sample with two times smaller Be doping in the **p** region. Again, the intensity of the sharp peak remained the same, while the size of the peaks in the phonon series were reduced by a factor of 2. The fact that this line is independent of the thickness and doping in the p-GaAs rules out the possibility that it arises from some sort of hot electron recombination in the GaAs. Using parameters from Table I, we calculated the

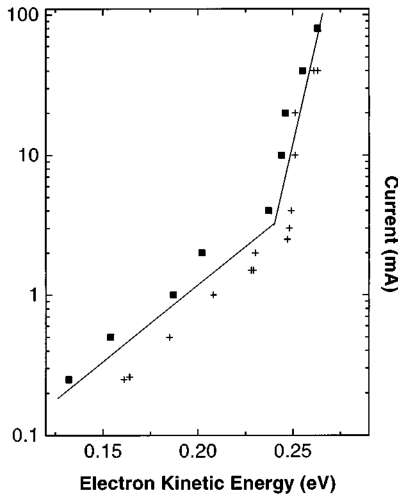

FIG. 11. The optical *I-V* curve of the 50 Å AlAs barrier sample, whose luminescence spectra are shown in Fig. 6. The solid lines are to guide the eye. The electron kinetic energy remains nearly constant for currents exceeding 2 mA.

energy of the quasibound X-point states in the barrier as a function of applied voltage. The observed shift of the line agrees with that calculated for the lowest X-point state. Lastly, we can estimate the luminescence intensity for such a transition which is indirect in both space and momentum. Following Ref. 23, the estimated indirect exciton radiative lifetime is about 30 μsec. The electron escape time from the X quantum well is in the order of 1 psec.[21] Thus the radiative recombination probability is about 3×10^{-7}. This can be compared with a 200 meV ballistic electron radiative recombination rate with a neutral acceptor in the **p** layer of about (10^{-6}).[7] Thus, the intensity of the indirect recombination between the AlAs and the GaAs and the ballistic electron peak intensity should be about the same order of magnitude. This is of course only a rough estimate, as the indirect recombination rate varies with surface roughness.[23] However, taken all together these measurements allow us, with reasonable confidence, to assign the sharp peak at about 1.78 eV to the indirect recombination of an electron trapped in the X valley in AlAs and a hole in the accumulation layer in GaAs. The energy of the peak is 10 meV higher than the energy of the real ballistic peak because the ballistic electron recombines with a 28 meV deep neutral acceptor, while the electron in the AlAs recombines with free holes in the hole accumulation layer, which is about 20 meV deep.

The fact that a ballistic electron peak above this indirect peak is not seen in Fig. 6 is also important. The absence of such a ballistic peak suggests that it is not possible to tunnel electrons through the AlAs when their energy exceeds that of the lowest quasibound state in the barrier. Apparently, the injected electrons scatter and thermalize within the AlAs before they can enter the GaAs. With this result it is also possible to understand the two slopes seen in Fig. 11. The slope at low currents corresponds to electrons tunneling below the quasibound state, and thus does reflect the change in tunneling probability with barrier voltage. At higher currents, however, the electron energy is clamped to state in the X valley of the GaAs, and the slope of the curve just measures how this state's energy changes with the applied bias.

C. Composite barriers

As mentioned earlier, the composite barrier structures allow us to ''fire'' electrons at the AlAs barrier with a range of energies, and thus see if it is possible for electrons to traverse the AlAs ballistically. Because of the low current density the bands can be assumed to be linear through the barrier. Thus, a tunneling electron gains considerable energy in the $Al_xGa_{1-x}As$ region. For a typical voltage range the kinetic energy obtained by the electron is expected to be between 60 and 250 meV. That is, the electron energy can easily exceed the X-valley energy of AlAs. Independent of the tunneling channel in the AlAs, Γ, or X, the maximum energy of the ballistic electrons appearing in the collector should be more than 300 meV if the transport is coherent (or even simply elastic).

The luminescence spectra of both composite barrier structures, Figs. 8 and 9, look much like the data for the simple AlAs barrier. The spectra are dominated by a sharp line between 1.75 and 1.8 eV, which shifts slowly towards higher energy as the current is increased. A clear phonon series can be seen in the spectra of both samples, which shows that energetic electrons are being injected into the GaAs. However, as mentioned earlier, the first, ballistic peak of this series can be seen to remain fixed as a low energy shoulder on the sharp line. In these respects the composite barrier samples appear much like the simple AlAs barrier, and our interpretation of the lines is the same. The large peak arises from indirect recombination of electrons in the AlAs and holes in an accumulation layer in the GaAs, while the phonon series consists of electrons which have thermalized within the AlAs to the lowest X-valley state, and then are injected into the GaAs with that energy. For the thinner composite barrier sample, with a 50 Å $Al_{0.3}Ga_{0.7}As$ layer, the sharp spectral line at about 1.74 eV disappears on the spectrum taken at 0.125 mA, which looks like the BELS spectra obtained for $Al_xGa_{1-x}As$ barriers. At this current the energy of the tunneling electrons lies below the lowest bound state in the X-valley quantum well. Thus the tunneling proceeds through a coherent channel in the low current regime.

Unlike the homogeneous tunnel barriers, spectra of the composite barrier devices do show lines at higher energies than the sharp indirect transition peak. In Fig. 8 there is a broad peak which shifts to above 1.8 eV, and then in the thicker sample (Fig. 9) a peak of presumably the same origin continues to shift with increasing current to about 1.95 eV. At high currents in the thick barrier sample there is a broad peak at 1.87 eV which does not tune with voltage and a second very broad line which tunes up to 2.1 eV, in some samples. At first glance one might think that these lines are produced by very energetic electrons being injected into the GaAs. However, if hot electrons are involved there should be a series of peaks separated by the LO phonon energy. There is no phonon series associated with these two lines. An explanation which does not involve energetic electrons in GaAs is needed. We believe that these lines are a consequence of hole tunneling, as discussed in the next section.

VI. HOLE TUNNELING

The peak at 1.87 eV has been found on a wide variety of composite barrier samples, always at the same energy. Its

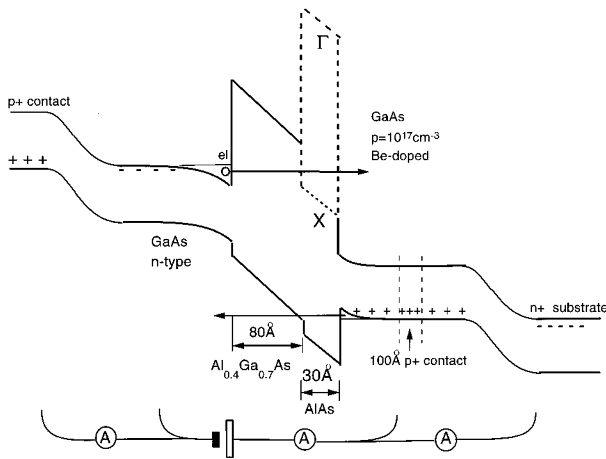

FIG. 12. Band digram of the four-terminal device with a composite barrier. All layers are contacted individually. The **p** layer is contacted through a 100 Å $p+$ contacting layer. The heavily doped substrate serves as one of the contacts. The voltage source is applied to the layers adjacent to the barrier.

energy coincides with the energy of holes at the minimum of the split-off valence band in GaAs recombining with free electrons.[3] The data suggest that hole, as well as electron, tunneling must be considered. Although the majority of holes in the accumulation layer will be heavy holes, the hole current is expected to consist mainly of light holes because of their larger tunneling probability. The light hole mass is comparable with the electron mass, while the tunnel barrier for holes is smaller. For example, for an $Al_xGa_{1-x}As$ ($x \leqslant 0.3$) barrier and assuming a 60:40 conduction:valence-band offset ratio, the barrier for holes is one-third less than that for electrons. However, the light hole fraction depends on the total density in the accumulation region and on the splitting between the light and heavy hole subbands. Detailed calculations show that the current of holes can be comparable to or even larger than the current of electrons for some sets of parameters.[11]

In order to distinguish between electron and hole tunneling we have employed a four-terminal device in which p-n junctions are used to separate the respective currents. The band and circuit diagram of these devices is sketched in Fig. 12. The composite tunnel barrier was inserted between an $n=2\times10^{17}$ cm^{-3} layer and a $p=1.5\times10^{17}$ cm^{-3} region, as in the previously discussed structures. Here, however, the active p-n structure is surrounded by another pair of p and n regions: a $p+$ layer ($p=2\times10^{18}$ cm^{-3}) on top of the n region, and an $n+$ layer ($n=1\times10^{18}$ cm^{-3}) below the p region and directly on the $n+$ substrate.

The structure was biased as shown in Fig. 12. The central p-n junction and tunnel barrier were forward biased, as in the previous structures. The outer pair of p-n junctions were shorted (through ammeters) and simply collected the tunnel-injected carriers. Holes which tunneled into the central n region diffused to the top junction, while electrons injected into the p layer diffused to the bottom junction, and their respective currents were measured. Some carriers may transport through these regions ballistically, or quasiballistically, but that will not affect the interpretation of the measured currents. The central p and n regions were made relatively

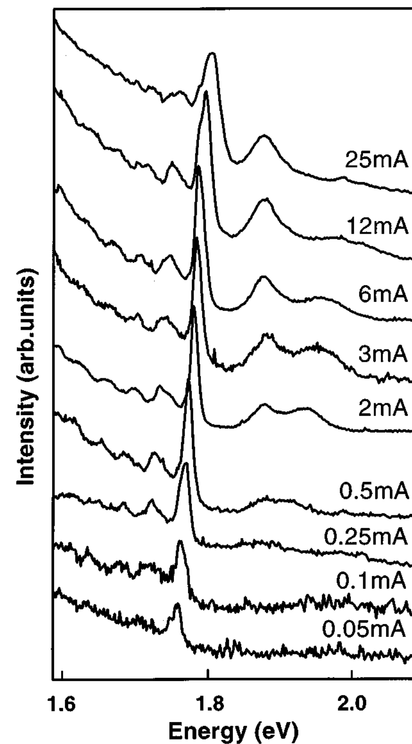

FIG. 13. BELS spectra of the four-terminal device. The spectra are similar to the ones obtained with previously described two-terminal composite barrier devices.

thick (0.5 μm) to enhance the luminescence. One difficulty is that acceptors in the central p region must be frozen out for BELS, but lateral voltage drops in this region would lead to nonuniform injection energies. We used a thin layer of a heavily p-doped GaAs (100 Å of $p=2\times10^{18}$ cm^{-3}) to provide lateral conduction, while the rest of the base could stay moderately doped. Mesa structures 100 μm wide were fabricated, and the electroluminescence was uniform over that area. This fact, as well as the absence of excessive line-broadening in the spectra, indicate that the lateral resistance of the conducting layers was small compared with the inter-layer resistance.

When the central p-n junction is forward biased, this device behaves like the composite barrier structures described above. Electroluminescence spectra for a range of currents are shown in Fig. 13. Again the spectra are dominated by a sharp line between 1.75 and 1.8 eV interpreted above as an indirect transition, and there is a phonon series at lower energies. At higher currents, a line appears at 1.87 eV as well as a broad line which continues to tune towards higher energy as the current increases.

Plotted in Fig. 14 are separate electron and hole currents and their sum (normalized to the total current), as a function of the total current through the tunnel barrier. In addition, since the hole collecting mesa on the top must be smaller than the n contact, the current has been normalized to this area. As can be seen, about 80% of the total current driven through the tunnel barrier was collected on one side or the other. This collection efficiency was sample dependent, ranging from 70% up to almost 100%. No attempt was made to passivate the surfaces of the mesas or otherwise optimize the collection efficiency.

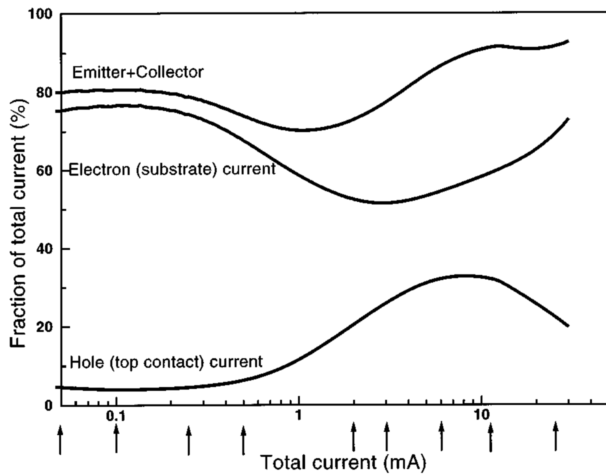

FIG. 14. Electrical characteristics of the four-terminal device. The electron current is measured as the substrate current when the voltage is applied to the barrier as sketched in Fig. 12. The hole current is the current of the top contact. The topmost curve is the sum of the currents of holes and electrons. The horizontal axis is the total current through the barrier. Marked with arrows are the currents for which the BELS spectra were obtained (Fig. 13).

Now it is possible to correlate the BELS spectra with these electrical measurements of the four-terminal device. The arrows on the bottom axis of Fig. 14 are the currents at which the BELS spectra in Fig. 13 were obtained. The hole current is negligible for total currents below about 1 mA, and the spectrum at 0.1 mA shows only the sharp indirect transition. Above 1 mA the hole component increases and reaches about half of the electron current. At the same time the luminescence line at 1.87 eV appears (the 0.5 mA spectrum), as well as the one which appears to move through it and to higher energy. This result supports our earlier suggestion that the 1.87 eV peak arises from hole injection into the n-GaAs. We suggest that this peak represents the recombination of holes thermalized in the spin split-off band with free electrons.

The highest energy peak which moves through the 1.87 eV line might be be related to an indirect in space recombination through the barrier, but its origin is not certain. It is very unlikely that it involves electron injection into the p-GaAs. First, the peak does not have a phonon series associated with it, nor does it have a low energy tail, which would be expected if the phonon peaks were simply smeared out by a broad injected distribution function, like that in the top spectrum in Fig. 4. If the peak were due to ballistic electron injection, then with such an energy the electron would be injected above X and L valleys of GaAs. These electrons could be either injected directly into the X or L valleys, or if injected into the Γ valley they would rapidly scatter to X and L, as seen in photoluminescence experiments.[3,24] The high energy luminescence peak in Figs. 9 and 13 could only arise from the small fraction of the electrons in the Γ valley, while the bulk of the electrons would thermalize within the X and L valleys and reenter the Γ valley with an energy of about 1.78 eV. The photoluminescence experiments[24] show that a series of "reentrant" peaks, about an order of magnitude more intense than the high energy peak in Figs. 9 and 13, should be produced, but we see no evidence for such a reentrant series.

The highest energy peak is also not likely to be related to ballistic hole injection because the donors will be ionized and the electrons near $\mathbf{k}=0$ are forbidden to recombine with ballistic holes by $\mathbf{k}$ conservation. Since the possibility that the peak originates from ballistic electrons or holes seems to be ruled out, we suggest that it arises from indirect (in space) recombination involving holes and electrons from the accumulation layers. Results in Sec. V show that the electron wave functions cannot extend through the AlAs above the X-point states, apparently due to scattering, and thus a spatially indirect process would depend upon the tails of the hole wave functions. Although the probability of such a recombination is extremely low, the probabilities of all the recombination processes addressed here are low. We can make an order of magnitude comparison between the intensity of the spatially indirect luminescence and that of holes at the top of the spin-orbit split-off band recombining with free electrons. During tunneling a hole might recombine with the electrons in the electron accumulation layer, at a rate determined by the amplitude of the wave functions. Both the spatially indirect recombination intensities and the hole tunneling current, which determines the split-off band luminescence, are proportional to the squared amplitude of the hole wave function at the electron accumulation layer, so hole wave-function amplitude should drop out in the comparison. In both cases then the recombination intensity is proportional to the product of electron and hole densities.

The hole split-off band luminescence is proportional to the product of the bulk electron density in the n side of the device (2×10^{17} cm^{-3}) and the average time that a hole spends at the top of the spin split-off band [about 0.3 psec (Ref. 3)]; numerically it is 6×10^{4} cm^{-3} sec. The spatially indirect recombination will also be proportional to the product of the electron and hole densities, but now the electron density is that of the accumulation layer (about 10^{12} cm^{-2} at these applied voltages). For a given current, the hole density within the barrier at the electron accumulation layer will depend on the hole wave-function amplitude and is inversely proportional to the hole velocity at the barrier, which is about 1.5×10^{8} cm/sec for light holes; numerically the product is 7×10^{3} cm^{-3} sec. This rough comparison of course ignores important considerations, such as the shape of both the electron and hole wave functions within the barrier and the fraction of injected holes which thermalize to the top of the split-off band before scattering to the light- or heavy-hole bands, but within these limitations it does suggest that the luminescence from these two processes should be comparable.

While both the intensity of this line and the hole component of the tunneling current appear to decrease above about 10 mA, it is not clear why. Quite possibly, Joule heating is responsible, since all of the luminescence features disappear with 50 mA of tunneling current.

VII. CONCLUSION

In summary we have used BELS to study electron and hole tunneling through AlAs, $Al_xGa_{1-x}As$ and composite barriers. The tunnel barrier is placed in the middle of a p-n junction, which is then forward biased. When electrons are

tunnel injected into p-GaAs, the luminescence provides a simple and accurate measure of the voltage across the barrier. We find excellent agreement between the ''optical'' I-V curves, in which the ''voltage'' is actually derived from the luminescence energy, and tunneling calculations for direct-gap barriers.

The situation can become more complicated for indirect gap barriers. In the case of an AlAs tunnel barrier the tunneling is similar to the direct-gap barrier as long as the tunneling electrons are below the lowest X-point state in the barrier. However, once the applied voltage is large enough for electrons to enter the conduction band of the AlAs, we are no longer able to observe coherent electron tunneling through the barrier. Rather, the electrons thermalize within the conduction band of the barrier and are either injected from the bottom of the X-point well into the GaAs, or undergo indirect (in both space and momentum) recombination with holes in the adjacent accumulation layer in the GaAs. These data clearly demonstrate that tunneling is a two-step incoherent process in this regime. In fact it is not only incoherent, but the tunneling electrons thermalize to essentially the band edge of the barrier before escaping into the GaAs. No $\Gamma \rightarrow \Gamma \rightarrow \Gamma$ tunneling through AlAs barriers has been observed in our experiments when the energy of electrons was higher than the X point of the barrier.

Composite barriers, with an $Al_xGa_{1-x}As$ region preceding an AlAs barrier, make it possible to tunnel electrons into the AlAs with energies well above the X-point states. Still no coherent or elastic transport through the AlAs can be seen. Again we find that the electrons thermalize within the AlAs and emerge at the energy of the lowest X-point state. At higher applied voltages a new luminescence line appears which we associate with hole tunneling and recombination within the n-GaAs. We confirmed the fact that hole tunneling grows dramatically at higher currents by separating injected carriers with p-n junctions. With a similar structure we have shown that there is a negligible hole current in the single $Al_xGa_{1-x}As$ barrier structures.

[*]Present address: Motorola, APRDL, Austin, TX 78721.

[1] M. Heiblum, M. I. Nathan, D. C. Thomas, and C. M. Knoedler, Phys. Rev. Lett. **55**, 2200 (1985).

[2] B. Brill, M. Heiblum, and H. Shtrikman, in *Proceedings of the 22nd International Conference on the Physics of Semiconductors, Vancouver, Canada, 1994*, edited by D.J. Lockwood (World Scientific, Singapore, 1995), Vol. 1, p. 241.

[3] B. P. Zakharchenya, D. N. Mirlin, V. I. Perel, and I. I. Reshina, Usp. Fiz. Nauk **136**, 459 (1982) [Sov. Phys. Usp. **25**, 143 (1982)].

[4] R. Beresford, L. F. Luo, W. I. Wang, and E. E. Mendez, Appl. Phys. Lett. **55**, 1555 (1989).

[5] C. L. Petersen, M. R. Frei, and S. A. Lyon, Phys. Rev. Lett. **63**, 2849 (1989).

[6] *Properties of Aluminium Gallium Arsenide*, edited by S. Adachi (Institute of Electrical Engineers, London, 1993).

[7] W. P. Dumke, Phys. Rev. **132**, 1998 (1963).

[8] R. Teissier, J. W. Cockburn, P. D. Buckle, M. S. Skolnick, J. J. Finley, R. Grey, G. Hill, and M. A. Pate, Phys. Rev. B **50**, 4885 (1994).

[9] R. Teissier, J. J.Finley, M. S. Skolnick, J. W. Cockburn, R. Grey, G. Hill, and M. A. Pate, Phys. Rev. B **51**, 5562 (1995).

[10] Y.K. Fukai, T. Furuta, and T. Ishibashi, Solid State Commun. **92**, 785 (1994).

[11] M. Fischetti, IEEE Trans. Electron Devices **38**, 634 (1991), and references therein.

[12] Jian-Bai Xia, Phys. Rev. B **41**, 3117 (1990).

[13] K. H. Gundlach, Solid State Electron. **9**, 949 (1966).

[14] H. Chaabane, M. Zazoui, J. C. Bourgoin, and V. Donchev, Semicond. Sci. Technol. **8**, 2077 (1993).

[15] E. L. Ivchenko, A. A. Kiselev, Y. Fu, and M. Willander, Phys. Rev. B **50**, 7747 (1994); Solid State Electron. **37**, 813 (1994).

[16] Y. Fu, M. Willander, E. L. Ivchenko, and A. A. Kiselev, Phys. Rev. B **47**, 13 498 (1993).

[17] D. Y. K. Ko and J. C. Inkson, Semicond. Sci. Technol. **3**, 791 (1988).

[18] D. Z.-Y. Ting and T. C. McGill, Phys. Rev. B **47**, 7281 (1993).

[19] T. Ando, S. Wakahara, and H. Akera, Phys. Rev. B **40**, 11 609 (1989); T. Ando and H. Akera, *ibid.* **40**, 11 619 (1989).

[20] K. Fujiwara, K. Kanamoto, Y. N. Ohta, Y. Tokuda, and T. Nakayama, J. Cryst. Growth **80**, 104 (1987).

[21] J. Feldman, J. Nunnenkamp, G. Peter, E. Göbel, J. Kuhl, K. Ploog, P. Dawson, and C. T. Foxon, Phys. Rev. B **42**, 5809 (1990).

[22] F. Stern and S. Das Sarma, Phys. Rev. B **30**, 840 (1984).

[23] A. Zrenner (private communication); R. Zimmermann and D. Bimberg, Phys. Rev. B **47**, 15 789 (1993).

[24] R. G. Ulbrich, J. A. Kash, and J. C. Tsang, Phys. Rev. Lett. **62**, 949 (1989).